High-Resolution Aerial Monitoring of Aquatic and Riparian Habitat in Selected Reaches of Wyoming's Powder River

April 1, 2008

A report of work completed June 2007 through March 2008

D.T. Booth and S.E. Cox
USDA Agricultural Research Service
Rangeland Resources Research Unit
High Plains Grassland Research Station
8408 Hildreth Rd
Cheyenne, WY 82009
307-772-2433

SUMMARY

Coalbed Methane (CBM) discharge water appears to have the potential to influence aquatic and riparian habitat through water volume and quality. Therefore, economical, but effective, means of monitoring for change in affected aquatic and riparian habitat is needed. We evaluated the utility of very-large scale aerial (VLSA) imagery for classifying riparian and aquatic habitat types using one aerial-sampling protocol. In related work we tested a new procedure for obtaining data from shadowed areas of images so as to increase the utility of nadir photos of shadow-producing vegetation; and, we explored ways of using VLSA with Aerocam and Quickbird imagery in a multi-spatial effort using VLSA to enhance the information available from the lower-resolution images (see figures). This was accomplished by developing new software that automatically creates world files for each VLSA image and allows the VLSA imagery to be displayed at the proper scale and location. The project also provided data for the BLM, National Operations Center (NOC) to test high-resolution stereo-based image modeling for change-detection capability. VLSA imagery was obtained in June, July, and August 2007 and image analysis completed in the subsequent 6 months. Measurements resulting from image analysis allow us to conclude that VLSA imagery can be used to measure percentage occurrence of specific aquatic habitat types using any date for emergent features and clear-water images for submerged types. We conclude that there is a need to alter our aerial-sampling protocol to obtain a greater portion of the channel length in our aerial sampling. VLSA is an effective means for monitoring riparian vegetation using the sampling methods employed in 2007. We found tamarisk (*Tamarix spp*.); a salt accumulating, desiccation-tolerant invasive alien species; currently has cover values comparable with the native cottonwood (*Populus fremontii*) at all 3 study sites for which VLSA imagery was obtained. We conclude that given the high percentage of emergent features of the Powder River channel, and the documented tamarisk succession scenarios of other western streams, that tamarisk poses an immediate threat to the aquatic habitat and native riparian vegetation. Will this threat will be exacerbated by unmanaged saline and sodic CBM outflows, or can managed CBM outflows be used as a tool for tamarisk control? We recommend further work to test these and related questions. Our test of a new procedure for obtaining data from shadowed areas was successful for ground photography but implementing the finding for aerial photography will require further work. We can immediately recommend the procedure for protocols using ground photography where shadows hide features being studied.

INTRODUCTION

Coalbed Methane (CBM) development produces large amounts of saline and sodic discharge water as a byproduct of methane extraction from subterranean coal seams. Water discharge rates vary from 5-15 gallons/minute/well, basin wide, resulting in an average discharge of 7,200 to 21,600 gallons/well/day. With current government permits allowing up to 51,000 CBM wells to be developed in the Powder River Basin by 2010, there is the potential for 360 million to 1.1 billion gallons/day of discharge water (403 to 1,232 acre feet/year), or up to 0.4% of the total normal-year flow of the Powder River. The effect of this increasing flow and water quality on the aquatic and riparian habitat of the river is unknown. The Powder River Aquatic Task Group (PRATG) seeks to monitor the river using methods capable of detecting and measuring ecologically important change to aquatic and riparian habitats downstream from CBM discharge.

Riparian surveys using 2-cm GSD (ground sample distance) very large scale (VLSA) imagery have demonstrated a higher sampling capability and lower cost than conventional ground-based monitoring—and have the advantage of creating a permanent photographic record (Booth and Cox 2006, and in preparation). This study addressed 4 objectives for repeat VLSA stereo imagery to be acquired over the Powder River at 3 selected monitoring sites: 1) evaluate the utility of the imagery for classifying riparian and aquatic habitat types, 2) evaluate the aerial sampling protocol used as a means for determining the extent of riparian and aquatic habitat types, c) investigate new procedures for obtaining data from shadowed areas, and d) work with BLM, NOC to test high-resolution stereo-based image modeling to facilitate the change-detection capability available from repeated VLSA imagery.

METHODS

Study Areas

Each study area was comprised of a 3.2-km (2-mile) stretch of the Powder River and adjacent riparian area, between the towns of Sussex and Arvada, Wyoming, characterized by sandy river channel substrate, cottonwood overstory and an annual grass understory with high tamarisk presence.

Above Pumpkin Creek – 406000 E,4863000 N; 1280 m elevation
Below Burger Draw – 407000 E, 4890000 N; 1250 m elevation
Above Crazy Woman – 409000 E, 4920000 N; 1189 m elevation

Image Acquisition

VLSA surveys are designed to systematically sample an area of interest by acquiring numerous images at regular intervals over the survey area (Booth and Cox, 2006). VLSA is a sampling tool, not a mapping tool. We used an externally-mounted dual-camera equipment module consisting of two digital SLR cameras (1Ds 11.1 megapixel with a 100mm, f/2.8 lens; 1DsMarkII 16.7 megapixel with an 840mm, image stabilized, f/5.6 lens; Canon USA, Lake Success, NY) set for 1/4000 sec. shutter speed, a Trackair navigation system (Trackair, Oldenzaal, Netherlands), an LD90-3100VHS-FLP laser rangefinder used as an altimeter (Riegl, Orlando, FL), a 401036 light meter (Extech, Waltham, MA) and a GPS16 WAAS-enabled GPS receiver (Garmin, Olathe, KS) (Fig. 1). Images were saved to 16 gigabyte compact flash cards (SanDisk, Milpitas, CA), and one laptop on board handled navigation. A 10-cm LCD screen

located near the pilot provided a graphic display of the flightlines and targets as planned using ArcGIS 9.0 (ESRI, Redlands,CA). The cameras were automatically fired by the navigation system and images and location data were captured concurrently. Altitude above ground level (AGL) and light intensity values were collected by a custom logger that simultaneously displayed the information for the pilot on the LCD monitor (Robert Berryman Consulting, Boulder, CO). Because of its capability for safe, slow flight (65-95 kph), we used a Moyes-Bailey Dragonfly powered by a Rotax 4-stroke, 115-horsepower turbocharged engine. The two-seat aircraft has a 10.5-m wing span and a US Federal Aviation Agency "Sport Airplane" designation. Images were saved as RAW files on both cameras, later converted to Tagged Image File Format (TIFF) images using Canon Digital Photo Professional 2.0. Both cameras were time-synchronized with the laptop prior to every flight, such that all images and metadata could be linked precisely by time. We used Merge software (Robert Berryman Consulting) to match images with GPS coordinates, altitude AGL, light intensity and ground speed, the latter two being predictors of image quality.

Imagery was obtained on June 15, July 10 and August 4, 2007, by completing 30 aerial transects, approximately perpendicular to the flow of the river, at each of the 3 reaches (Fig. 2). Stereo imagery was obtained using programmed flight lines with trigger impulses at 2-second intervals from 250-m above ground level (AGL) to yield 60% forward overlap. Images were inspected for quality and clarity after each flight, and on one occasion re-flown to meet quality standards.

Image Analysis

Channel Wetted Width

Channel wetted width and open-water width was measured at up to 20 equidistant points in the image (fewer points if the river channel did not extend across the entire image, as in a curve) using ARS-developed *ImageMeasurement* software (Booth et al. 2006a). Additionally, counts were made for each image of the percentage of transects that intercepted an emergent feature, and of the number of times each transect crossed from a wetted area to a dry area within the channel. Both serve as indices of habitat complexity, with higher numbers of emergent features indicating higher aquatic habitat complexity.

Occurrence of Aquatic Habitat Types and Riparian Vegetation

Two separate meetings with Paul Dey and Anna Senecal were held 3 Dec. 2007 and 19 February 2008 to define aquatic habitat types they felt could be classified from the imagery. As a result of these meetings, the aquatic habitat was classified as follows: emergent dry, puddles, backwater, island, debris, isolated pool, dry channel, shallow, wave form and variable-depth flow. Classification was completed on one 2-cm GSD image/transect (the image directly over the channel) at all three sites for all three dates. It was noted that because the aerial imagery did not present a continuous image of the river channel, features such as shoals and some backwaters could not be identified. Additionally, the imagery did not allow for classification of runs, pools and riffles because those habitat types are defined by water depth and/or substrate composition, features which cannot easily be assessed from aerial imagery. Riparian area above the waterline was classified into the following categories: cottonwood (*Populus fremontii*), willow (*Salix spp.*), tamarisk (*Tamarix spp.)*, sagebrush (*Artemisia spp.*), rabbitbrush (*Chrysothamnus spp.* (synonym: *Ericameria*)), Russian olive (*Elaeagnus angustifolia*), grass/grasslike, cactus

(*Opuntia spp.*), forb, annual (consisting primarily of senesced downy brome (*Bromus tectorum*) and annual mustards (*Descurainia* and *Sisymbrium spp.*)), leafy spurge (*Euphorbia esula*), bare ground, woody litter, litter, rock, cattle dung and man-made features/items. Classification was completed on two 2-mm GSD images/transect (on either side of the channel, or in the case of an upland-vegetated bluff on one side, two images on one side of the channel) at all three sites for the July collection date. July was chosen because tamarisk plants were blooming and more easily distinguished from surrounding vegetation relative to other collection dates.

ARS-developed *SamplePoint 1.37* (Booth et al 2006b) was used to measure aquatic habitat as a percentage of the June image high water mark, and the 17 categories of riparian ground cover. SamplePoint software facilitated point-sampling of imagery at 100/points/image.

Multi-spatial Analyses

Although not a part of the proposed work, the authors participated with Gretchen Meyer (WY State Office, BLM) and Robert McDougal (USGS) in exploring ways to use VLSA resolutions with Quickbird and Aerocam imagery. Seamless integration of VLSA imagery into a GIS framework is hampered by a lack of georeference inherent with VLSA imagery. We cooperated with Robert Berryman (Independent Programmer) to create software that automatically creates world files for each VLSA image, allowing display of VLSA imagery at the proper scale and location, although not necessarily in the proper orientation. We then explored using ArcMAP to rubbersheet VLSA imagery to Aerocam images that were georeferenced by the BLM NOC, which in turn, are aligned with Quickbird imagery.

Shadow Mitigation

For the August flight, an additional Canon 1Ds MII camera with 100mm lens was acquired and mounted adjacent to the identical camera/lens already on board. The additional camera was set to acquire images with an exposure compensation of +2 stops, meaning that all images it acquired would be overexposed. Images from the two Canon 1Ds MII cameras were paired, then used to create high dynamic range (HDR) images using Photomatix Pro 2.4 (HDR Soft, Monpellier, France) . The resulting tone-mapped HDR images were composites of the two original images, and used details from one image to fill in areas lacking detail in the other, such as in shadowed or overexposed areas.

To follow up the aerial experience we conducted a ground study using a 12.8-megapixel digital SLR camera with 28-90mm f/4.0-5.6 lens mounted on a 2-m-tall aluminum camera frame such that 0.8-mm ground sample distance (GSD) nadir images could be acquired from 2-m above ground level (Booth et al. 2004). Camera operation in auto-bracket mode resulted in capture of three RAW-format images of varying exposure for every station: Normal, 2 stops underexposure and 2 stops overexposure. Aperture-priority mode (f/8) was used so that the exposure varied only by shutter speed, thus keeping the relatively-high depth of field constant across all bracketed images. Digital ISO (gain) was set to 200. Twenty-five plots were systematically photographed in this manner on a sunny morning in early fall with sun angle of ~30º at the High Plains Grasslands Research Station, Cheyenne, WY. RAW images of the normal (uncompensated) exposure for each plot were converted to TIF images. RAW images were also used to batch-create HDR images within Photomatix Pro 2.4 (HDR Soft, Montpellier, France) by combining each set of 3 images/plot into a single HDR file, then applying tone mapping to create a TIF image that drew detail from all three. Resulting HDR images were saved as TIF files, and were largely free of areas that were too dark or washed out. SamplePoint 1.37

(Booth et al. 2006b) was used by 5 different users to manually measure cover from both the TIF and HDR images, by means of manual classification of 100 points/image, in order to test the hypothesis that HDR images allow cover information to be extracted from areas that are normally too dark to analyze in a normal TIF image.

Stereo Modeling

This will be reported by BLM, NOC.

RESULTS AND DISCUSSION

Acquisition

VLSA imagery was acquired of 5,390 targets across all sites and collection dates. Complete image metadata and analysis results are available in the supplemental file: PR ATG 2008 Report Supplement.xls.

Channel Wetted Width

Channel wetted widths and open-water widths were greatest in June and lowest in July (Fig. 3). August values were generally greater than July except at APC, where July and August values were equal. Wetted width was approximately equal to open water width at all sites in June, but appreciably larger in July and August due to more emergent features. The percentage of transects/image that intercepted an emergent feature was lowest in June (highest flow) and highest in July (lowest flow) (Fig 4). At APC, nearly 60% of all transects laid across the channel encountered an emergent feature. The Complexity Index was highest in July at low flow, and lowest in June at high flow (Fig 4). Complete results are found in PR ATG 2008 Report Supplement.xls.

Occurrence of Aquatic Habitat Types and Riparian Vegetation

The percentage occurrence of aquatic habitat types is largely a function of river flow with emergent features, islands, debris, dry channels and other flow-affected types of habitat becoming more prevalent (greater percent occurrence) at lower flows (Fig. 5). Submerged types such as wave form and shallow are evident and can be measured when the water is clear. Turbid water, such as encountered on the June and August collection dates, made the classification of features involving water depth (shallow or wave-form) impossible, leading to a blanket classification of almost all wetted areas as variable-depth flow. This, in turn, led to the appearance of a large increase of shallow and wave-form areas during July (Fig. 5), when water was clear, but this apparent increase was primarily due to turbid water preventing accurate classification of these features in June and August. Because of this, we conclude that remote sensing of the Powder River should be conducted only during periods of clear water. Dey and Senecal concluded that images acquired through aerial transects perpendicular to the channel limited their ability to judge and classify some aquatic habitat, such as backwaters and shoals. They suggested that a survey method resulting in more data along the channel is needed.

The documentation of the percent occurrence of each aquatic habitat type and ground cover—particularly cover of key species of riparian vegetation (Fig. 6) —establishes photographic baselines against which future monitoring efforts can be compared. In the case of riparian vegetation, this baseline seems especially important with respect to tamarisk, which if

left uncontrolled will likely alter the riparian plant community and the Powder River channel (PR ATG 2008 Report Supplement.xls). Channel alteration by tamarisk is a well-documented process of channel narrowing by encroachment from the banks and by colonization of bare emergent aquatic features such as islands and bars (Graf 1982, Birken and Cooper 2006). The high number of emergent features noted in the section Channel Wetted Width, give an indication of the features of the Powder River channel that might support a channel-changing tamarisk encroachment. Birken and Cooper (2006) suggest the greatest tamarisk recruitment in their lower Green River study area occurred during a sequence of large annual floods followed by years of low flows. Specifically, their recruitment models showed that high peak flows were a statistically-significant predictor of high recruitment success (high seedling establishment). However, Birken and Cooper (2006) also cite evidence that large floods which follow tamarisk germination and establishment increased tamarisk seedling mortality due to erosion and prolonged inundation.

Tamarisk is a salt accumulating, desiccation-tolerant (Arndt et al. 2004, Campbell and Strong 1964, Mace 1971) invasive alien shrub or tree that currently has cover values comparable with the native cottonwood at all 3 study sites for which VLSA imagery was obtained in 2007 (Fig. 6). Does the salt-tolerant characteristic of tamarisk mean it will have a greater competitive advantage over native species if unmanaged CBM outflows increase the salinity or sodicity of soil substrates? Will unplanned CBM outflows enhance tamarisk recruitment through seed dissemination and periodic, but limited, high flows insufficient to cause tamarisk seedling mortality? Conversely, the evidence that floods increase tamarisk seedling mortality (Birken and Cooper 2006) raises the question of whether CBM outflow might be managed to appropriately enhance natural floods and whether that enhancement can be used to maintain desired channel features and retard tamarisk recruitment. The answers to these questions have important implications for the future of the Powder River, its riparian corridor and associated wildlife species.

Multi-spatial Analyses

We found that there are enough features visible in Aerocam, and to some extent, Quickbird, to match control points with VLSA imagery. The technique which seemed to work best involved creating world files for each VLSA image, displaying those images in ArcMAP over the Aerocam layer, then rubbersheeting each VLSA image using control points in the Aerocam image. Since the Aerocam imagery is georeferenced, the resulting georeferenced VLSA image also lined up reasonably-well with Quickbird satellite imagery, resulting in a multi-spatial GIS framework which may facilitate classification training of Quickbird imagery with VLSA imagery (Fig. 7). The process, however, does take 8-10 minutes/image, and is an impractical method for geo-referencing thousands of images.

Shadow Mitigation

Image analysis of ground-based images revealed that merging several images into a single HDR image significantly changed cover measurements as it improved clarity of shadowed areas (Fig. 8). On an individual user basis, the number of points classified as shadow was always lower in HDR images, and the number of points classified as saturated was usually lower when classifying HDR images. Across all users, shadow decreased 24.3%, and saturated points decreased 2.0% with HDR classification ($P<0.001$, $n=5$ users); however, the effects for some cover classes were dependant on the user, as seen in significant interaction between user and

image type (Table 1). The 26% reduction in the number of points that could not be classified because of darkness/brightness resulted in increases of measured green grass (7.7%), brown grass (3.6%), litter (5.7%), rock (0.5%) and bare ground (5.0%). This demonstrates that HDR imagery has the potential to increase cover-classification accuracy, and provides a completely new strategy for dealing with shadows in remote sensing imagery.

Aerial HDR images suffered from two problems. Acquiring two images that encompassed the exact same field of view from two different cameras on a moving platform turned out to be much more difficult than anticipated. Merging two misaligned images, even if misaligned by only inches, or a degree of rotation around the lens axis, resulted in blurry and distorted HDR composites (Fig. 9). Secondly, large wildfires in western and central Wyoming during the flight caused inordinately hazy conditions, obscuring sunlight and softening shadows such that the August images had much less shadow to correct for than images from June or July. Thus, even with slightly blurry HDR images, shadow attenuation was minor because there was very little shadow to begin with (Fig. 9). This was the first attempt at HDR image generation from a moving platform that we know of, and served an important role in defining future research objectives in order to tackle this problem.

CONCLUSIONS

The 2007 VLSA surveys again demonstrated the capability of this technology to provided higher-resolution imagery at lower cost than is available from other commonly-used platforms. With respect to Objective 1, we conclude that VLSA imagery can be used to measure percentage occurrence of the aquatic habitat types (as defined by Paul Dey and Anna Senecal) using any date for emergent features and only dates with clear-water images for submerged types. With respect to the riparian vegetation, we conclude that tamarisk is a threat to the aquatic habitat of the channel and to existing native riparian vegetation. As to Objective 2, we conclude that there is a need to alter our aerial surveys to obtain a greater portion of the channel length in our sample imagery. Objective 3 was to determine if new procedures could be developed for obtaining data from shadowed areas. This was accomplished; however, implementation of the finding for aerial photography will require substantial further work, therefore, the new methods will not find immediate application to Powder River aerial surveys.

ACKNOWLEDGEMENTS

The research was funded by a grant to D.T. Booth from the US Department of Interior, Bureau of Land Management, National Operations Center with funds obtained from the Powder River Aquatic Task Group. The authors thank Joe Nance of Cloud Street Flying Services, who piloted the aircraft for data collection; Carmen Kennedy, who performed much of the image analysis; and Matt Bobo, Gretchen Meyer, and Robert McDougal for sharing lower-resolution imagery, and for their contributions to the multi-spatial analyses.

LITERATURE CITED

Arndt, S.K., C. Arampatsis, A. Foetzke, X. Li, F. Zeng, and X. Zhang**.** 2004. Contrasting patterns of leaf solute accumulation and salt adaptation in four phreatophytic desert plants in a hyperarid desert with saline groundwater. Journal of Arid Environments 59:259-270.

Birken, A.S. and D.J. Cooper. 2006. Processes of *Tamarix* invasion and floodplain development along the lower green river, Utah. Ecological Applications, 16(3), 2006, pp. 1103–1120.

Booth, D. T., S.E. Cox, M. Louhaichi, and D.E. Johnson. 2004. Lightweight camera stand for close-to-earth remote sensing. Journal of Range Management 57:675-678.

Booth, D.T., and S.E. Cox. 2006. Very-large scale aerial photography for rangeland monitoring. Geocarto International 21(3):27-34.

Booth D.T., S.E. Cox, and R.D. Berryman. 2006a. Precision measurements from very large scale aerial digital imagery using ImageMeasurement, Laserlog, and Merge software applications. Environmental Monitoring and Assessment 112: 293–307.

Booth D.T., S.E. Cox, and R.D. Berryman. 2006b. Point sampling digital imagery using 'SamplePoint'. Environmental Monitoring and Assessment 123:97-108.

Booth, DT, SE Cox and G Simonds. 2007. Riparian monitoring using 2-cm GSD aerial photography. Ecological Indicators 7:636-648.

Booth, DT, SE Cox, G Simonds and E. Sant. In prep. Riparian change detection from 2-cm GSD aerial imagery.

Campbell, C. J. and J. E. Strong. 1964. Salt Gland Anatomy in Tamarix Pentandra (Tamaricaceae). The Southwestern Naturalist 9:232-238.

Graf, W.L. 1982. Tamarisk and river-channel management. Environmental Management 6: 283-296.

Mace, A.C. Jr. 1971. Osmotic Water Stress: Mesophyll Saturation Deficit and Transpiration Rates of Tamarisk. The Southwestern Naturalist 16:117-120.

Table 1. Significance probability values from a two-way Analysis of Variance that measured the effect of HDR image enhancement against control normal images (Treatment), and user effects, across 9 classification categories (User). The test was based on 25 HDR images and 25 normal images classified by 5 users into 9 classification categories. Where significant, the cover difference between HDR and control normal images is given as the deviation from controlnormal (Difference). User ×x Treatment interaction is given, first with all 5 users (Interaction), and then with anomalous data from a single user removed for those classes that showed significant interaction (Interaction with anomalous data removed). Classes that did not show significant user × treatment interaction were not run again with anomalous user data removed.

Class	Treatment	User	Interaction	Difference	Interaction with anomalous user data removed
Green Grass	<0.0001	0.013	0.7928	7.7 ± 3.7	.
Brown Grass	0.0024	0.0012	0.0527	3.6 ± 5.0	.
Forb	0.8763	0.0002	0.9997	.	.
Litter	<0.0001	<0.0001	0.0979	5.7 ± 6.1	.
Rock	0.0251	<0.0001	0.5299	0.5 ± 0.9	.
Bare Ground	<0.0001	<0.0001	0.1592	5.0 ± 6.2	.
Shadow	<0.0001	<0.0001	<0.0001	-24.3 ± 8.3	0.45
Saturated	<0.0001	<0.0001	0.0046	-2.0 ± 3.0	0.41
Unknown	<0.0001	<0.0001	<0.0001	3.6 ± 4.6	<0.0001

Figure 1. Images were acquired using two digital cameras on board a Moyes-Bailey Dragonfly light aircraft. Individual components are labeled and described in text.

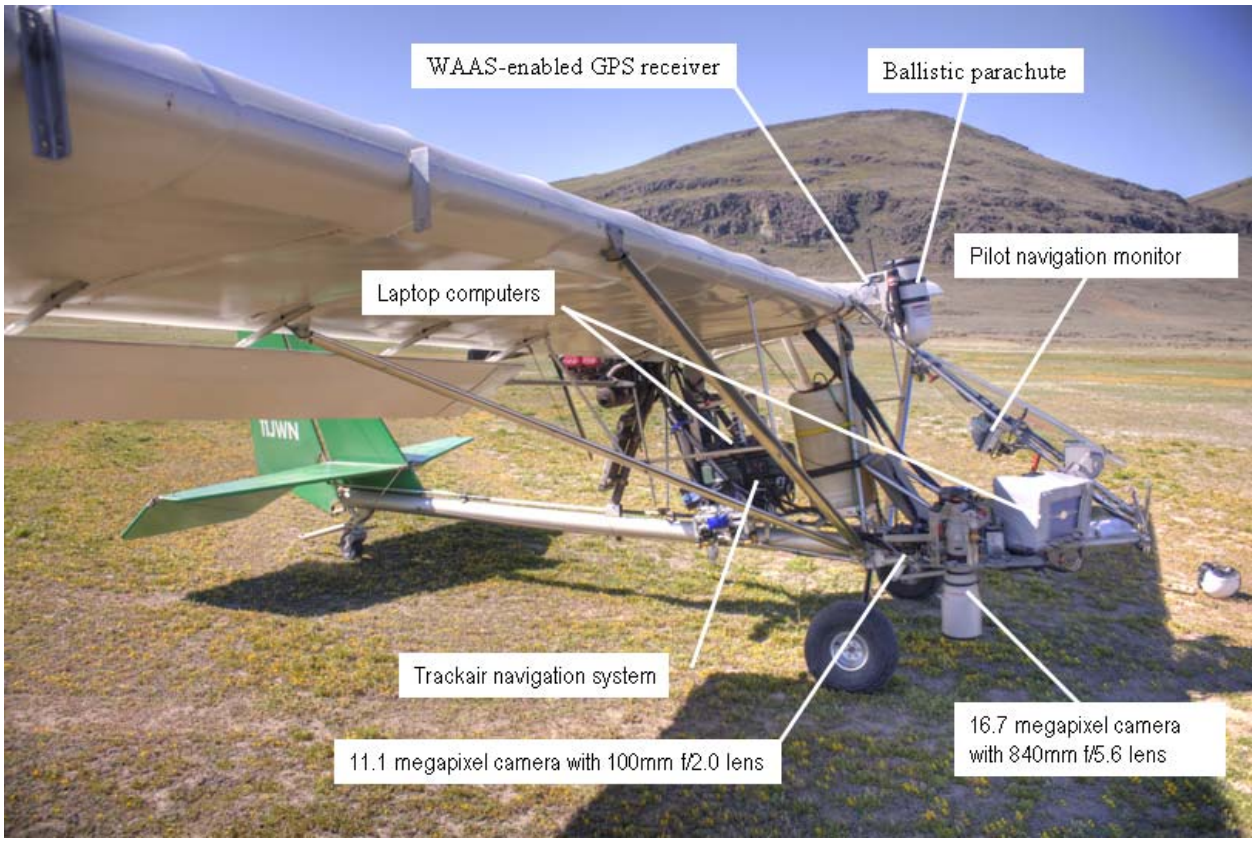

Figure 2. Sample sites along the Powder River are highlighted by orange triangles at *Above Pumpkin Creek* (APC), *Below Burger Draw* (BBD), and *Above Crazy Woman* (ACW). Sampling flight lines and image trigger points are shown in enlarged inlays.

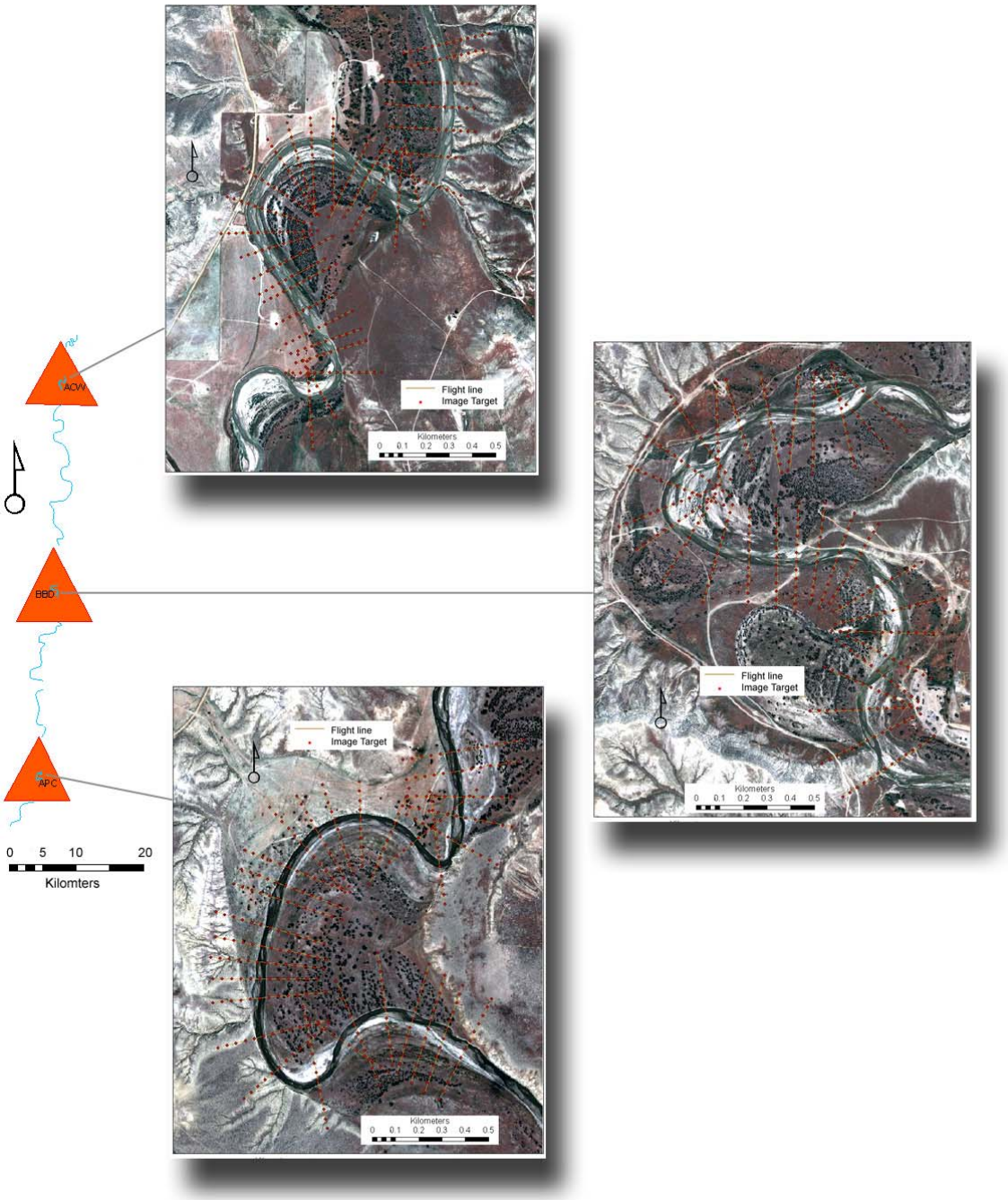

Figure 3. Channel wetted width, which is inclusive of emergent features (A) and open water width, which is not inclusive of emergent features (B), measured from all sites (ACW = Above Crazy Woman, APC = Above Pumpkin Creek, BBD = Below Burger Draw) for June, July and August.

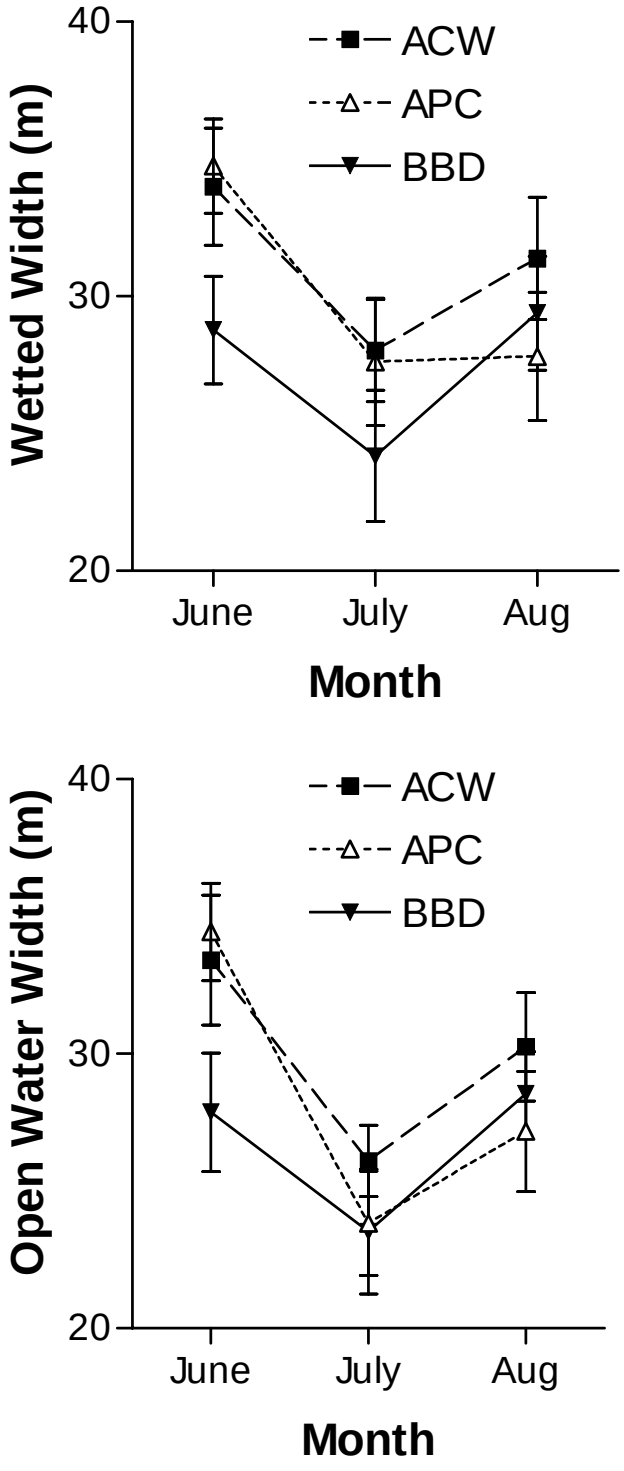

Figure 4. Number of transects which intercepted an emergent feature (A), and mean number of times, per image, that each transect crossed a wetted/dry boundary within the channel (B), at all three sites (ACW = Above Crazy Woman, APC = Above Pumpkin Creek, BBD = Below Burger Draw) for June, July and August. Both serve as indices of aquatic habitat complexity.

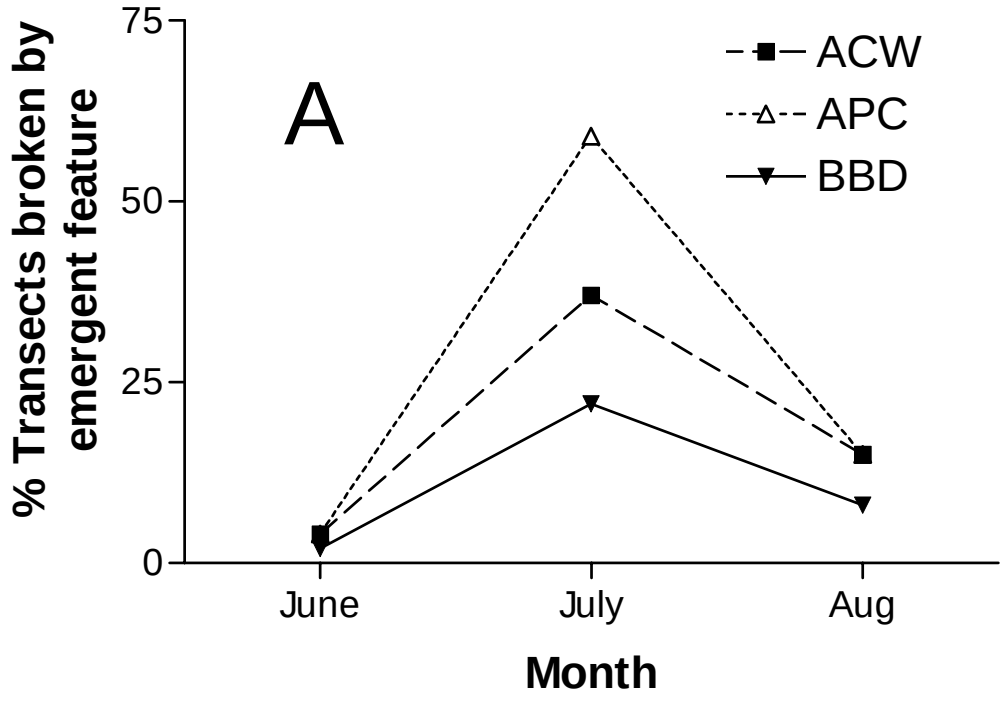

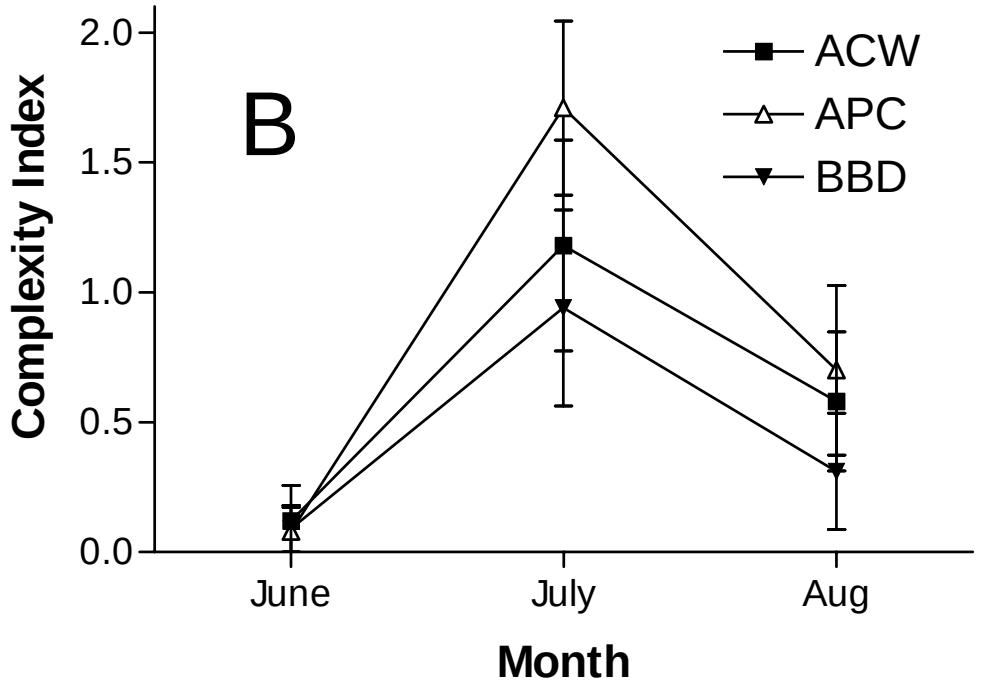

Figure 5. Aquatic habitat types from Below Burger Draw in June, July and August.

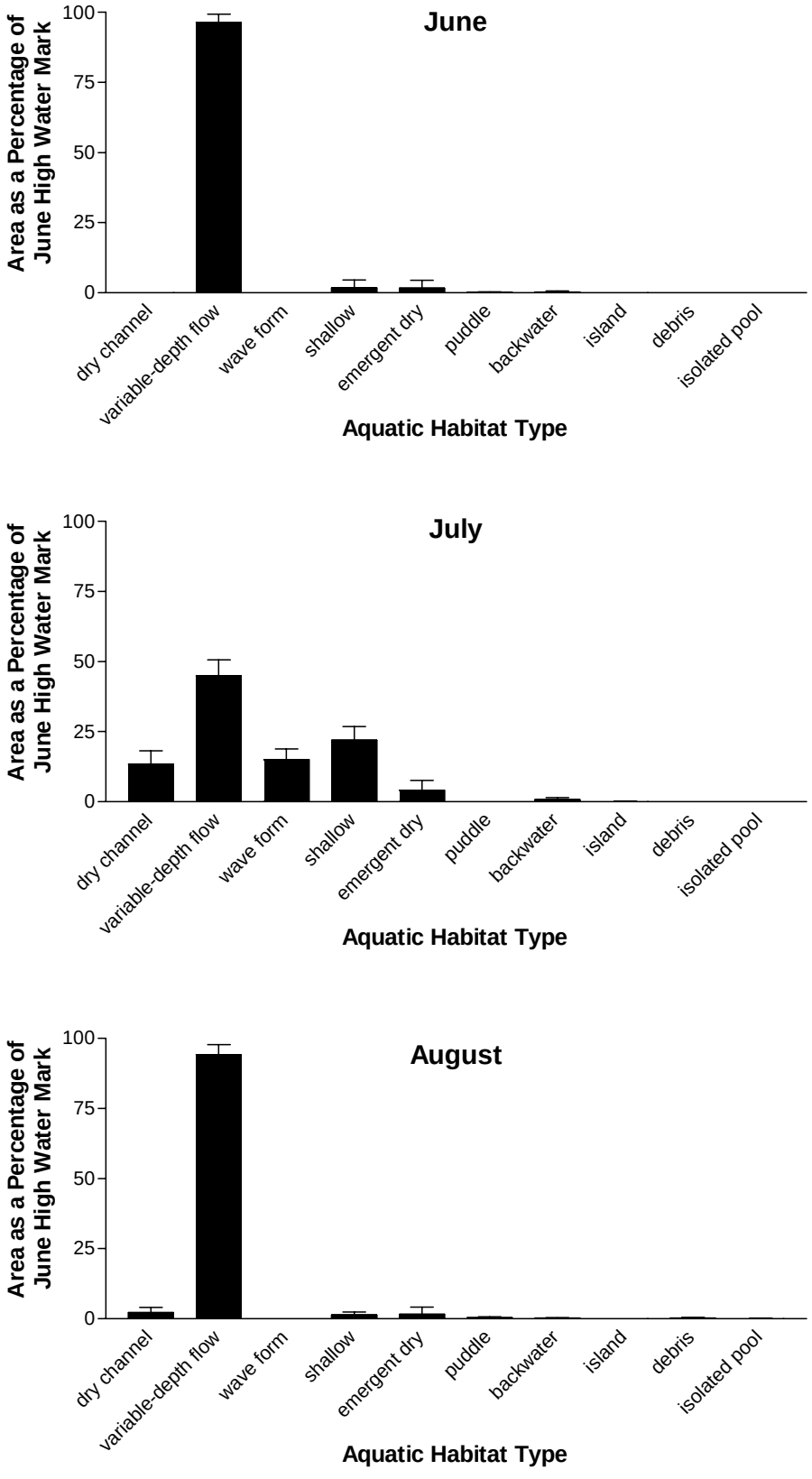

Figure 6. Riparian area vegetation cover measurements from all study sites in July.

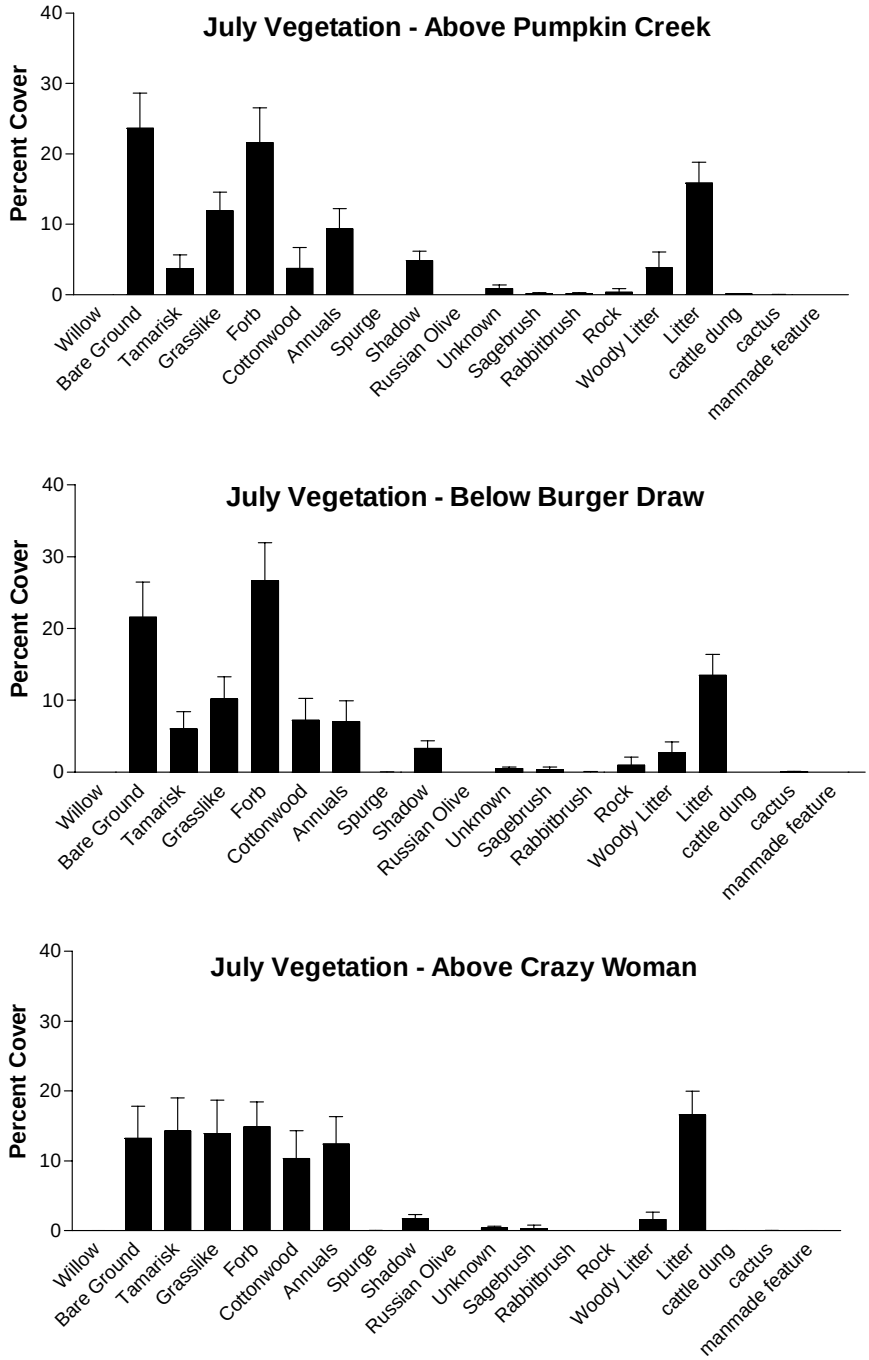

Figure 7. Two georeferenced VLSA images overlaid on a Quickbird scene of the ACW site. Detail from the VLSA images may help to train classification of Quickbird imagery, which spans a greater area than the VLSA imagery.

Figure 8. Original image of a 1m^2 plot acquired from 2m above ground level on left, with high dynamic range composite image of the same plot on the right showing increased clarity and detail in shadowed and overexposed areas.

Figure 9. Original VLSA image acquired from 250m above ground level (top), with high dynamic range composite image of the same view (bottom) showing misalignment of images and shadow attenuation that is much less pronounced than in Figure 7. Thick atmospheric haze obscured the sun during collection, diminishing shadows and reducing the effect of extending the dynamic range. White arrows show area of greatest shadow mitigation in the scene.